Microscopic optical potentials for Li isotopes

Wendi Chen[1,], *Hairui* Guo[2,*], *Weili* Sun[2,], *Tao* Ye[2,], *Yinlu* Han[3,], and *Qingbiao* Shen[3,]

[1]Graduate School of China Academy of Engineering Physics, Beijing 100088, China
[2]Institute of Applied Physics and Computational Mathematics, Beijing 100094, China
[3]Key Laboratory of Nuclear Data,China Institute of Atomic Energy, Beijing 102413, China

Abstract. The microscopic optical potentials for Li isotopes (A=6,7) without free parameter are obtained by folding the microscopic optical potentials of their internal nucleons with density distributions generated from corresponding internal wave functions of Li isotopes. An isospin-dependent nucleon microscopic optical potential based on the Skyrme nucleon-nucleon effective interaction is used as the nucleon optical potential. Shell model is employed to construct the internal wave functions of Li isotopes and derive their density distributions of internal nucleons. The Li microscopic optical potentials are used to calculate the elastic-scattering angular distributions and reaction cross sections. The results reproduce experimental data well and are comparable to those calculated by phenomenological optical model potentials in many cases.

1 Introduction

The microscopic optical potential (MOP) has great significance in nuclear reaction theory and astrophysics. It is derived from nucleon-nucleon interaction theoretically and need not adjust its parameters to fit experimental data. Moreover, it can give guidance for nuclear reaction, especially in the research involving interaction systems without or lack of scattering measurement.

Nuclear reactions involving Li isotopes have been a subject of great interest for decades, not only because of their application in isotopes production and nuclear astrophysics, but also for the reaction mechanism as they are all well-known weakly bound nuclei [1]. However, the scattering experimental data for them is not abundant. Therefore, microscopic optical potentials for Li isotopes will be useful to understand the reaction mechanism and analyze those nuclear reactions.

In the present work, the MOPs for Li isotopes are obtained by folding the MOPs of its constituent nucleons with their density distributions. An isospin-dependent nonrealistic nucleon MOP derived by using the Green's function method based on the Skyrme nucleon-nucleon interaction is applied to be the MOP for internal nucleon. Shell model is used to construct the internal wave function and generated the nucleon density distributions. In order to evaluate the predictive power of the MOPs, they are used to calculate the elastic-scattering angular distributions and reaction cross sections and the calculated results are compared with those calculated by a phenomenal global optical potential (GOP) and experimental data .

This paper is organized as follow: the theoretical models and formulas of the MOPs are presented in Sec. 2; the calculated results and analysis are given in Sec. 3; the conclusions are drawn in Sec. 4 finally.

2 Theoretical model

Folding model is a common method to get the optical model potential of complex nucleus, in which the potential for the whole nucleus is considered to be the sum of its internal nucleons or clusters. Hence, the MOPs for the Li isotopes are expressed as

$$U(\vec{R}) = \int U_n(\vec{R}+\vec{r})\rho_n(\vec{r}) + U_p(\vec{R}+\vec{r})\rho_p(\vec{r})d\vec{r}, \quad (1)$$

where

$$\int \rho_n(\vec{r})d\vec{r} = N; \int \rho_p(\vec{r})d\vec{r} = Z. \quad (2)$$

U_n and U_p are the MOPs of neutron and proton from Ref. [2, 3] respectively. They are an isospin-dependent nonrealistic microscopic optical potential for nucleon base on Skyrme nucleon-nucleon effective interactions. Different Skyrme parameters, SGOII [4] and SKC16 [2], are used to obtain the MOPs of internal nucleons for ^{6}Li and ^{7}Li respectively. The incident energy of each nucleon is assumed to be the total incident energy multiplied by $1/A$. $\vec{R}$ is the relative coordinate between the center of mass of target and projectile. ρ_n and ρ_p are the density distributions of neutron and proton of Li isotopes respectively. ρ_n and ρ_p are derived from the ground state internal wave function of Li, Φ_{gs}, directly and are expressed as

$$\rho_{n(p)}(\vec{r}) = \left\langle \Phi_{gs} \left| \sum_{i=1}^{A} \delta(\vec{r}-\vec{r}_i)\delta_{\tau_{n(p)},\tau_i} \right| \Phi_{gs} \right\rangle, \quad (3)$$

where $\vec{r}_i$ is the coordinate of ith nucleon of Li relative to the center of mass of the projectile and τ_i is its isospin. τ_n and τ_p are the isospins of neutron and proton respectively.

*e-mail: guo_hairui@iapcm.ac.cn

Table 1. The parameters of ρ_n and ρ_p derived from shell model. The value of r^m_{rms} are taken from Ref. [1]

	^{6}Li	^{7}Li
r^m_{rms} (fm)	2.54	2.50
β (fm^{-2})	0.2454	0.2743
a_n (fm^{-3})	0.0567	0.0921
b_n (fm^{-5})	0.0058	0.0081
a_p (fm^{-3})	0.0567	0.0621
b_p (fm^{-5})	0.0058	0.0076

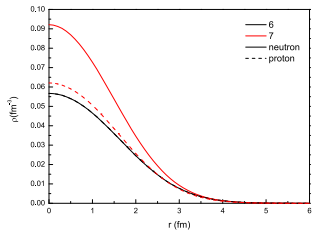

Figure 1. The density distributions of neutron (ρ_n) and proton (ρ_p) of Li isotopes. The solid lines and dash lines represent ρ_n and ρ_p respectively. The black and red lines donate the results of ^{6}Li and ^{7}Li respectively.

The internal wave function of Li isotopes could be constructed in the manner of shell model. As we only concern the properties of nucleus in the ground state, a full $0\hbar\omega$ harmonic oscillator space, $(1s)^4(1p)^{A-4}$, is used to obtain Φ_{gs}. Hence, it is expressed as

$$\Phi_{gs} = \mathcal{A}\left\{\sum_{LS}\prod_{i=1}^{A}\varphi_i(\vec{r}_i)\zeta\right\}, \tag{4}$$

where $\mathcal{A}$ is the antisymmetric operator and φ is harmonic oscillator wave function. ζ represents the spin and isospin part. $\sum_{LS}$ represents the summation for all functions which meet the requirements of total angular momentum by LS coupling method.

ρ_n and ρ_p derived from Eq. (3) and (4) have a unified form as

$$\rho_{n(p)}(\vec{r}) = \left(a_{n(p)} + b_{n(p)}r^2\right)\exp\{-\frac{A}{A-1}\beta r^2\}. \tag{5}$$

β=$m\omega/\hbar$ is the harmonic oscillator constant and its value is determined by the matter root mean square radius r^m_{rms} [1]. The parameters are listed in Table 1 and the density distributions are plotted in Fig. 1.

Furthermore, the spin-orbit coupling potential of the MOP, U^{so}, is calculated in a similar way with Eq. (3), while the effect of the nucleon-nucleus interaction should be taken into account, as U^{so} contributes mainly in the surface region of target nucleus. The nucleon spin-orbit coupling potential, U^{so}_n for neutron and U^{so}_p for proton, taken from Ref. [2] should be multiplied with m^*/m, where m^* is the nucleon effective mass inside the target nucleus. Hence, U^{so} is expressed as

$$U^{so}(\vec{R}) = \int \frac{m^*_n}{m_n}U^{so}_n(\vec{R}+\vec{r})\rho_n(\vec{r}) + \frac{m^*_p}{m_p}U^{so}_p(\vec{R}+\vec{r})\rho_p(\vec{r})d\vec{r}. \tag{6}$$

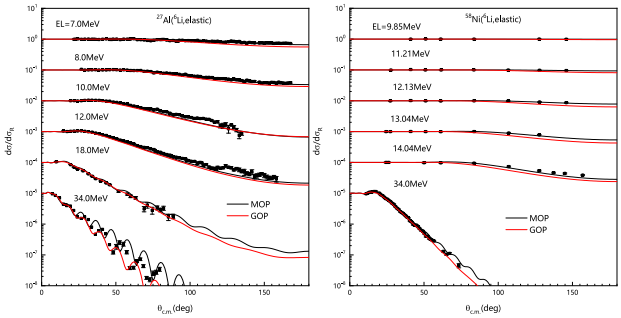

Figure 2. Calculated elastic scattering angular distributions in the Rutherford ratio of ^{6}Li for ^{27}Al and ^{58}Ni targets compared with experimental data [7, 8, 10, 11]. The black and red lines represent the results calculated by the MOP and GOP [5] respectively.

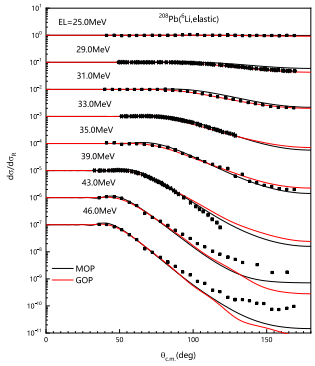

Figure 3. Same as Fig. 2 but for ^{208}Pb target. The experimental data are taken from Ref. [9].

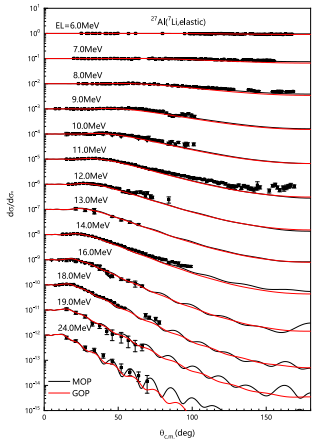

Figure 4. Same as Fig. 2 but for ^{7}Li projectile and ^{27}Al target. The experimental data are taken from Refs. [12, 13]. The GOP is taken from Ref. [6].

3 Calculated result and discussion

Based on the MOPs of Li isotopes, elastic scattering angular distributions and reaction cross sections are calculated below 100 MeV. Moreover, comparison with global optical potential [5, 6] and experimental data is made in order to evaluate their predictive power.

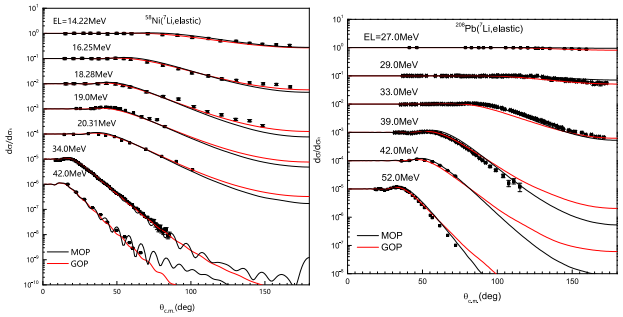

Figure 5. Same as Fig. 2 but for ^{7}Li projectile and ^{58}Ni, ^{208}Pb target. The experimental data are taken from Refs. [14–18]. The GOP is taken from Ref. [6].

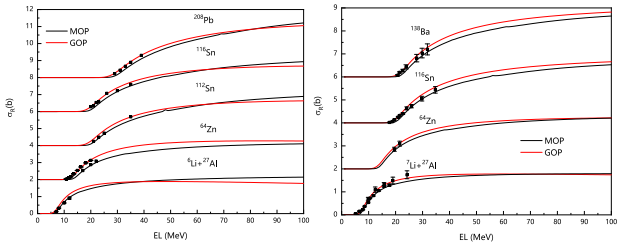

Figure 6. Reaction cross sections for ^{6}Li and ^{7}Li. The black and red lines represent the results calculated by the MOPs and the GOP [5, 6]. The experimental data are taken from Refs. [18–27].

Fig. 2 presents the calculated elastic scattering angular distributions of ^{6}Li for ^{27}Al and ^{58}Ni targets. For ^{27}Al, the results calculated by the MOP have a reasonable agreement with the experimental data [7, 8], while the GOP works better overall. A underestimation and overestimation for the MOP occur at EL=12.0 MeV and EL=34.0 MeV in the large angle respectively. Oppositely, the MOP performs better than the GOP for ^{58}Ni and gets a good agreement with experimental data [10, 11].

The calculated elastic scattering angular distributions of ^{6}Li for ^{208}Pb are plotted in Fig. 3. A better agreement has been obtained by the MOP at EL≤39 MeV than the GOP, while both of them underestimate the experimental data [9] at EL=43.0 and 49.0 MeV.

The divergence with experimental data for the ^{6}Li MOP may be resulted from the lack of breakup effect, which is not taken into account in the process of generating the MOP. On the contrary, the breakup effect are grossly involved in the GOP as its parameters had been adjusted to fit the scattering data. Therefore the results calculated by the GOP are relatively closer to the measured value.

Similar calculations are made for ^{7}Li and presented in Figs. 4 and 5. A satisfying agreement with experimental data [12–18] is obtained by the MOP.

Moreover, reaction cross sections, σ_R, are calculated for ^{6,7}Li at EL≤100 MeV and plotted in Fig. 6. Reasonable agreements with experimental data [18–27] for MOPs are obtained. However, a gradual worsening of predictions for ^{6}Li reaction cross sections has been noticed, especially for relatively heavier target. For example, the cross sections for ^{6}Li and ^{208}Pb reaction calculated by the MOP are about 150mb less than the experimental data at EL=30-40 MeV, while the MOP reproduce correct cross sections for ^{6}Li + ^{27}Al around EL=10 MeV. On the other hand, the reaction cross sections of ^{6}Li calculated by the MOP are smaller than those calculated by the GOP at low incident energies. σ_R is expressed as

$$\sigma_R = -\frac{2}{\hbar v}\langle \chi^+ | W | \chi^+ \rangle , \tag{7}$$

where χ^+ represents the outgoing wave, W is the imaginary part of the optical potential and v is the relative velocity of target and projectile in center of mass frame. A stronger W of the MOP, relative to the real part of the MOP, is needed to obtain correct σ_R for heavy target nucleus at low incident energies. Breakup effect is expect to generate this correction, as it can provide an absorptive contribution to the imaginary part of optical potential and a repulsive contribution to the real part [28].

4 Conclusion

The microscopic optical potentials for Li isotopes without free parameter are obtained by folding model base on Skyrme nucleon-nucleon effective interaction. Shell model is used to construct the internal wave functions of Li isotopes. The elastic scattering angular distributions and reaction cross sections for targets from ^{27}Al to ^{208}Pb at incident energies no more than 100 MeV are calculated by the Li isotopes microscopic optical potentials. Generally, the MOP obtained can well reproduce the elastic scattering angular distributions and performs better than the GOP in some cases, especially for ^{7}Li. The MOPs can both reproduce the reaction cross sections reasonably. The divergence with experimental data is expect to be solved or impaired by taking the breakup effect into account, which will be our next subject.

References

[1] Kuterbekov, K. A., Kabyshev, A. M. and Azhibekov, A. K., Chinese J. Phys. **55**, 25232539 (2017).
[2] Y. Xu, H. Guo, Y. Han, and Q. Shen, EPJ Web of Conferences **146**, 12021 (2017).
[3] Q. Shen, Y. Han, and H. Guo, Phys. Rev. C. **80**, 024604 (2009).
[4] J. Treiner and H. Krivine, J. Phys. G **2**, 285 (1976).
[5] Xu, Y. et al. Phys. Rev. C **98**, 116 (2018).
[6] Yongli, X. et al. Phys. Rev. C **97**, 014615 (2018).
[7] J.M.Figueira et al. Nucl. Phys. A **787**, 484 (2007).
[8] G.Ciangaru, R.L.Mcgrath and F.E.Cecil, Nucl. Phys. A **380**,147 (1982).
[9] Zhang C L , Zhang H Q , Lin C J , et al. Chin. Phys. Lett. **23**, 1146 (2006).
[10] E.F.Aguilera et al. Phys. Rev. C **79**, 021601 (2009).
[11] K.D.Veal et al. Phys. Rev. C **60**, 064003 (1999).
[12] J. M. Figueira et al., Phys. Rev. C **73**, 054603 (2006).
[13] K. Kalita et al., Phys. Rev. C **73**, 024609 (2006).

[14] C. W. Glover, R. I. Cutler, and K. W. Kemper, Nucl. Phys. A **341**, 137 (1980).
[15] A. Andronic, Nucl. Phys. A **661**, 333 (1999).
[16] K. Zerva et al., Eur. Phys. J. A **48**, 102 (2012).
[17] P. Clark et al., Nucl. Phys. A **349**,258 (1980).
[18] A. M. M. Maciel et al., Phys. Rev. C **59**, 2103 (1999).
[19] E. A. Benjamim, et al., Phys. Lett. B **647**, 30 (2007).
[20] M. Zadro, et al., Phys. Rev. C **80**, 064610 (2009).
[21] M. G. Saint-Laurent, et al., Z. Phys. A: At. Nucl. **332**, 457 (1989).
[22] P. R. S. Gomes, et al., Phys. Rev. C **71**, 034608 (2005).
[23] N. N. Deshmukh, et al., Eur. Phys.J.A **47**, 118 (2011).
[24] N. Keeley, et al., Nucl. Phys. A **571**, 326 (1994).
[25] P. R. Gomes, et al., Phys. Rev. C **71**, 1 (2005)
[26] K. Kalita, et al., Phys. Rev. C **73**, 024609 (2006).
[27] E. Benjamim, et al., Phys. Lett. B **647**, 30 (2007).
[28] Y. Sakuragi, M. Yahiro, and M. Kamimura, Progress of Theoretical Physics Supplement, **89**, 136 (1986)